Available online at www.sciencedirect.com
ScienceDirect
Nuclear Physics B Proceedings Supplement 00 (2014) 1–6
Nuclear Physics B Proceedings Supplement

Electroweak Physics at LHCb

Stephen Farry
On behalf of the LHCb collaboration
Department of Physics, University of Liverpool, L69 7ZE, United Kingdom

Abstract

The LHCb forward acceptance covers a range of rapidities not accessible by the other LHC experiments, allowing for complementary measurements. We report recent measurements of electroweak boson production, either inclusive, or in association with a jet or a D meson.

Keywords:
electroweak physics, forward physics

1. Introduction

The LHCb detector [1] is a single-arm forward spectrometer instrumented in the pseudorapidity region $2 < \eta < 5$ and optimised for the study of B and D mesons. While it shares some of its coverage with the ATLAS and CMS detectors at the LHC, the unique forward coverage of the detector means that it can perform precision tests of the Standard Model (SM) in a region inaccessible to the other experiments.

Measurements of W and Z production cross-sections at the LHC constitute an important test of the SM. While the partonic cross-sections are well understood and known to the percent level, additional theoretical uncertainties arise due to the knowledge of the Parton Density Functions (PDFs) which parameterise the behaviour of the partons within the colliding protons. The pseudorapidity coverage of LHCb allows it to probe these PDFs in a distinct region of (x,Q^2) space, where x is the fraction of the proton momentum carried by the parton, and Q is the energy transfer of the interaction. Consequently, precision measurements of electroweak boson production at LHCb can provide important constraints to the PDFs in a unique kinematic region. The (x, Q^2) coverage of the LHCb detector at $\sqrt{s} = 7$ TeV, as well as other experiments is shown in Fig. 1.

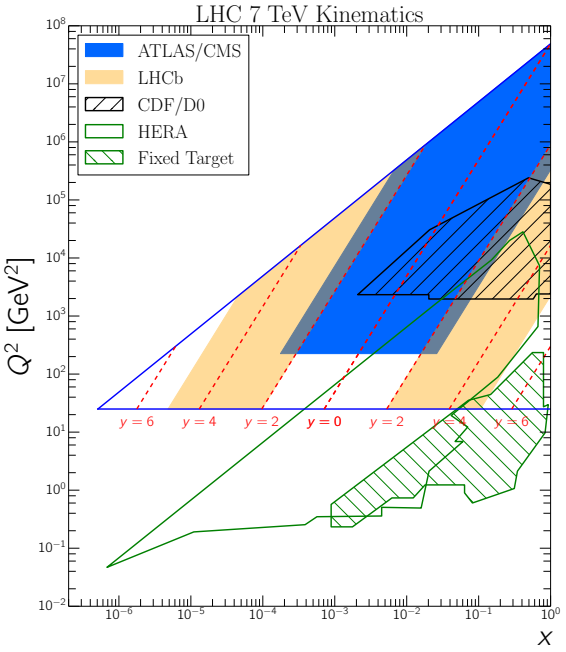

Figure 1: The (x, Q^2) plane and where it is covered by experiment. The LHCb detector covers two distinct regions at low- and high-x

2. Inclusive W boson production

A measurement of inclusive W boson production at $\sqrt{s} = 7$ TeV is performed at LHCb using the muonic decay mode of the W boson and the full dataset collected by the LHCb detector in 2011 corresponding to an integrated luminosity of approximately 1.0 fb^{-1} [2]. Events are selected which contain a triggered, reconstructed and identified muon with a transverse momentum exceeding 20 GeV/c lying in the pseudorapidity region between 2 and 4.5. In addition, the muon is required to be consistent with production at the primary vertex, and to be isolated from other event activity. The event is also required not to contain any additional muons with a $p_{\rm T}$ greater than 2 GeV/c.

The signal purity is obtained by fitting the $p_{\rm T}$ spectrum of the selected data sample in eight bins of muon pseudorapidity to the expected background and signal shapes, which are obtained from a combination of data and simulation.

The expected background contributions are: the decay-in-flight of pions and kaons, the semi-leptonic decay of heavy-flavour mesons, $Z \to \mu\mu$ events where one of the muons is not reconstructed in the LHCb acceptance and $Z \to \tau\tau$ events containing a single muon in the final state. A total of 806094 W candidates are selected, with signal purities of 77.13% and 77.39% for the positively and negatively charged candidates respectively. The result of the template fit for the full pseudorapidity range is shown in Fig. 2. The fit residuals show an imperfect description of the data by the adopted templates, particularly at high transverse momentum, however the effect on the signal yield is small.

The $W \to \mu\nu$ production cross-section is measured by correcting the signal yield for losses due to reconstruction and selection efficiency, acceptance and final-state radiation (FSR). The reconstruction and selection efficiencies are primarily measured using data-driven techniques while the acceptance and FSR corrections are determined from simulation. The cross-sections are calculated in the fiducial region defined by the kinematic selection, where the muons have a transverse momentum exceeding 20 GeV/c and a pseudorapidity between 2 and 4.5. The total cross-sections for W^+ and W^- production in the fiducial range are measured to be

$$\sigma_{W^+\to\mu^+\nu} = 846.9 \pm 2.0 \pm 10.9 \pm 29.9\text{pb},$$
$$\sigma_{W^-\to\mu^-\nu} = 664.6 \pm 1.8 \pm 8.7 \pm 23.5\text{pb}$$

where the first uncertainty is statistical, the second is systematic and the third is due to the luminosity. The

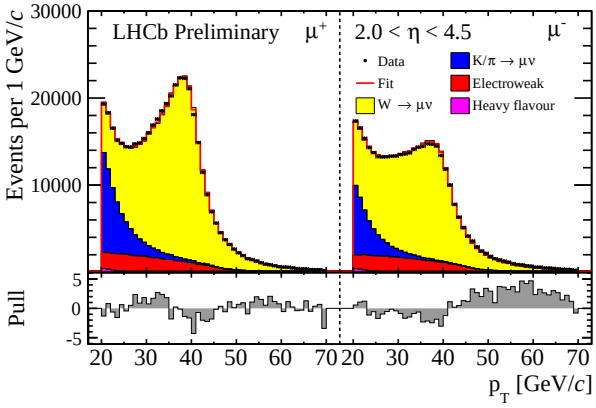

Figure 2: Tranverse momentum distribution of positively (left) and negatively (right) charged $W \to \mu\nu_\mu$ candidates in the total pseudorapidity range, and the corresponding signal and background contributions determined from the template fit.

W^+ and W^- cross-sections as a function of muon pseudorapidity are presented in Fig. 3 with their asymmetry shown in Fig. 4. Many experimental and theoretical uncertainties cancel in the measurement of the asymmetry which provides a precision test of the SM. The measurements are compared to theoretical predictions calculated at next-to-next-to-leading order (NNLO) in QCD using different parameterisations of the PDFs. The results are in general good agreement with the predictions, with the rate of W^- production is seen to overtake that of W^+ production at large lepton pseudorapidity. This result supersedes the measurement performed with 37 pb^{-1} of data collected in 2010 [3] with an improvement in systematic uncertainties of almost a factor of three. The measurement presented here has also subsequently being updated with a reduced luminosity uncertainty of 1.71% in Ref. [4].

3. Forward Z+jet production

The production of a Z boson in association with a hadronic jet is studied at LHCb using the di-muon decay channel of the Z with 1.0 fb^{-1} of data collected at $\sqrt{s} = 7$ TeV in 2011 [5]. Events are selected containing a pair of oppositely charged muons fulfilling the same kinematic requirements as those in the inclusive W analysis but with the added requirement that the di-muon invariant mass, $M_{\mu\mu}$, should satisfy $60 < M_{\mu\mu} < 20$ GeV/c^2. In addition the event is required to contain a high-$p_{\rm T}$ jet with a pseudorapidity of between 2 and 4.5. Two different $p_{\rm T}$ thresholds are considered for the jet, where it is required to have a transverse momentum in excess of 10 or 20 GeV/c. The jets are reconstructed

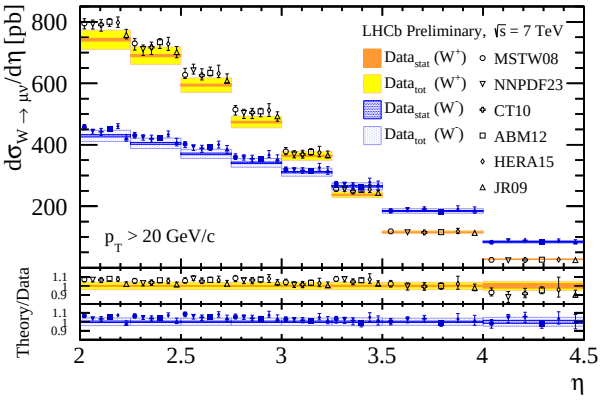

Figure 3: Differential W^+ and W^- cross-sections as a function of muon pseudorapidity.

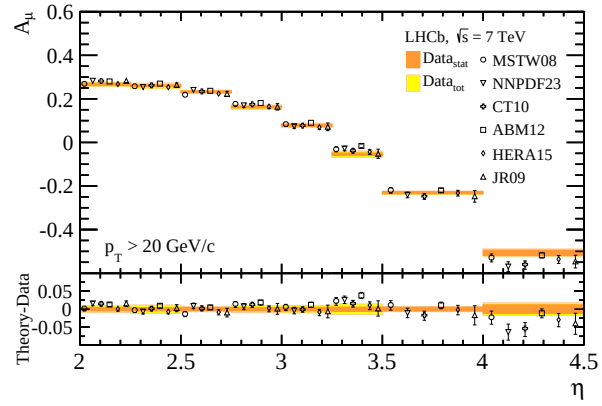

Figure 4: Lepton charge asymmetry presented as a function of muon pseudorapidity.

using an anti-k$_T$ algorithm [6] with distance parameter $R = 0.5$. Reconstructed tracks and deposits in the electromagnetic and hadronic calorimeters serve as charged and neutral inputs to the jet reconstruction algorithm and are selected using a particle flow algorithm. Quality requirements are also placed on the jet to reduce the number of fake jets; the jet should contain at least two particles matched to the same interaction point as the Z boson, at least one track in the jet should satisfy $p_{\rm T} > 1.8$ GeV/c and no single track should carry more than 75% of the jet energy. The jet energy scale is determined using simulation and cross-checked in data, with the jet energy resolution varying between 10-15% for the $p_{\rm T}$ range between 10 and 100 GeV/c. The purity of the samples selected with both jet $p_{\rm T}$ thresholds is approximately 99.7%, consistent with that reported in the inclusive $Z \to \mu\mu$ analysis [3]. The fraction of $Z \to \mu\mu$ events containing a jet are determined to be

$$\frac{\sigma(Z + \text{jet})}{\sigma(Z)} = 0.209 \pm 0.002 \pm 0.015$$

for jet $p_{\rm T} > 10$ GeV/c and

$$\frac{\sigma(Z + \text{jet})}{\sigma(Z)} = 0.083 \pm 0.001 \pm 0.007$$

for the jet $p_{\rm T} > 20$ GeV/c threshold. The first uncertainty is statistical and the second is systematic. Differential cross-sections normalised to the inclusive Z cross-section for the 20 GeV/c $p_{\rm T}$ threshold are presented as a function of the Z boson $p_{\rm T}$ in Fig. 5 and as a function of the azimuthal separation of the Z boson and the jet, $\Delta\phi$, in Fig. 6. The measured cross-sections are compared to theoretical predictions at up to $O(\alpha_s^2)$ with parton showering and hadronisation effects included and show general good agreement. As expected, the calculations performed at $O(\alpha_s)$ fail to describe the $|\Delta\phi|$ distribution to high accuracy.

4. Z boson production in association with a D-meson

The $Z \to \mu\mu$ selection is also applied to search for the production of Z bosons in association with D mesons in the full 2011 dataset [7]. Charged and neutral D mesons are reconstructed using the channels $D^0 \to K^\mp\pi^\pm$ and $D^\pm \to K^\pm\pi^\mp\pi^\pm$ where the final states are required to be in the invariant mass ranges $1.82 < M_{K^\mp\pi^\pm} < 1.92$ GeV/c^2 and $1.82 < M_{K^\pm\pi^\mp\pi^\pm} < 1.91$ GeV/c^2. The D meson candidates are further required to be consistent with the same primary vertex as the Z candidate, to have a $p_{\rm T}$ between 2 and 12 GeV/c,

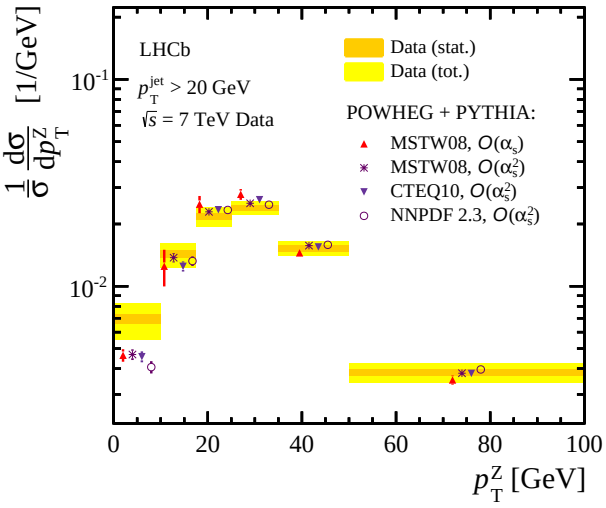

Figure 5: The normalised differential cross-section for Z+jet production as a function of the transverse momentum of the Z boson

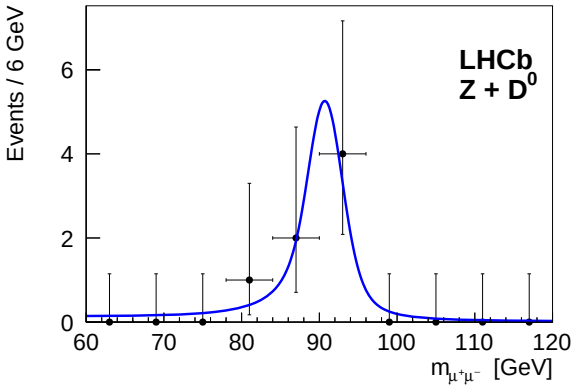

Figure 7: The reconstructed Z boson mass for events selected in the $Z + D^0$ final state.

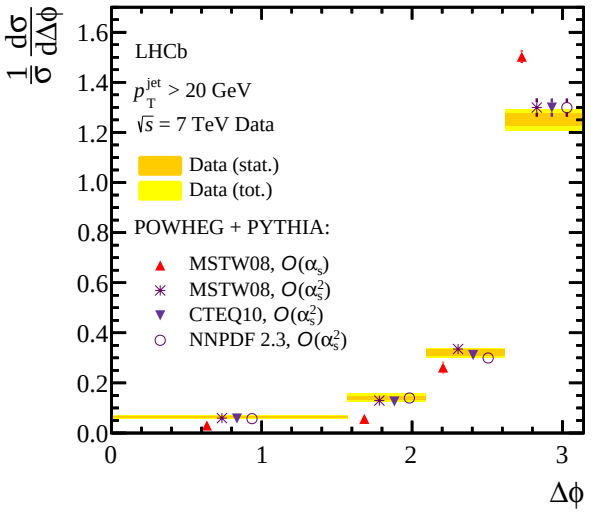

Figure 6: The normalised differential cross-section for Z+jet production as a function of the azimuthal separation of the jet and the Z boson.

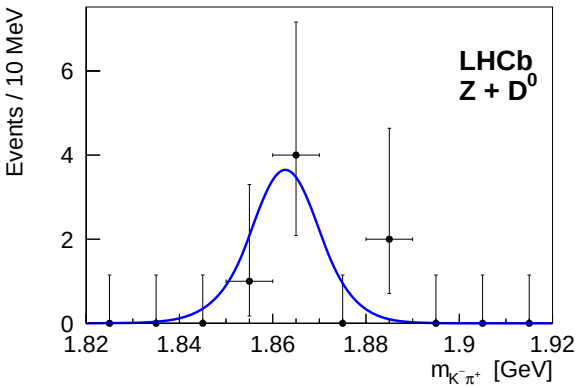

Figure 8: The reconstructed mass of the D meson for events selected in the $Z + D^0$ final state.

and a rapidity between 2 and 4. Backgrounds are considered from the feed-down from beauty meson decays, combinatorics, and pile-up where the Z boson and the D meson are produced in different proton-proton interactions. The signal purity is determined to be approximately 95% for both decay modes of the D. A total of 7 candidates are selected in the $Z + D^0$ decay channel and 4 in the $Z + D^{\pm}$ decay mode, corresponding to a combined significance of 5.1 standard deviations. The reconstructed masses of the Z boson and the D^0 meson for events selected in the neutral channel are shown in Figs. 7 and 8. The cross-section for Z boson production in association with neutral and open charm mesons is measured to be

$$\sigma_{Z\to\mu^+\mu^-,D^0} = 2.50 \pm 1.12 \pm 0.22\text{pb},$$

$$\sigma_{Z\to\mu^+\mu^-,D^+} = 0.44 \pm 0.23 \pm 0.03\text{pb}$$

where the first uncertainty is statistical and the second is systematic. The cross-sections receive contributions from processes where the Z and D meson are production in the same partonic interaction, and where they are produced in separate interactions, known as single- and double-parton scattering respectively. The latter production mechanism dominates and the combined results are seen to be in agreement with theoretical predictions for the $Z+D^0$ channel but lower than predictions for the $Z+D^{\pm}$ channel. However, due to the large statistical uncertainties in the measurement, no definitive conclusion can be drawn.

5. Z boson production in proton-lead collisions

A search for Z boson production is performed using a dataset corresponding to 1.6 nb^{-1} collected by the LHCb collaboration in proton-lead collisions at a centre-of-mass energy per nucleon pair of $\sqrt{s_{NN}}$ = 5 TeV at the start of 2013 [8]. The measurement is performed using both forward (proton-lead) and backward (lead-proton) collisions. The standard $Z \to \mu\mu$ selection is applied to the dataset with the background contributions from muon mis-identification and the decay of heavy flavour mesons determined using data-driven methods. A total of 15 candidates are selected with a purity of 99.74±0.06%. This gives a significance of 10.4σ for the Z signal in the forward direction and 6.8σ for the backward direction. The di-muon invariant mass of the candidates in the forward direction is shown in Fig. 9. The measurements are compared to theoretical predictions calculated at NNLO using the FEWZ generator [9] and computed with and without considering nuclear effects based on the EPS09 nuclear PDF set [10].

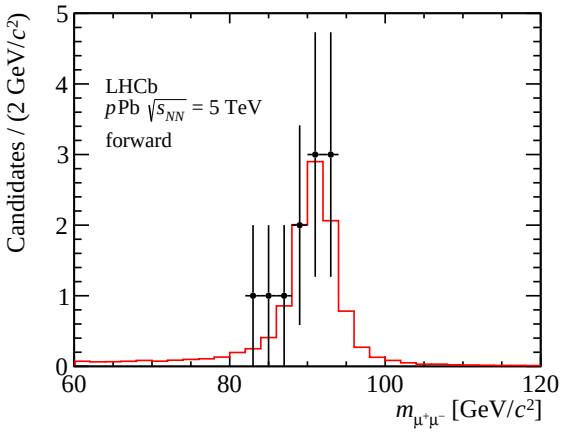

Figure 9: The di-muon invariant mass of the $Z \to \mu\mu$ candidates in proton-lead collisions in the forward direction. The simulated shape, normalised to the number of selected events, is indicated by the red line.

The resultant comparison is shown in Fig. 10. In addition, the ratio of Z boson production in the forward and backward direction, R_{FB}, is measured in the common rapidity region between 2.5 and 4.0 and determined to be

$$R_{\rm FB}(2.5 < |y| < 4.0) = 0.094^{+0.104}_{-0.062}(stat.)^{+0.004}_{-0.007}(syst.)$$

where the first uncertainty is statistical and the second is systematic. The 99.7% (i.e. 3σ) confidence interval with symmetric coverage is [0.002, 1.626] where the asymmetry of the interval around the central value is due to non-Gaussian statistical uncertainties. The probability to observe a value of $R_{\rm FB}$ no larger than that measured in the absence of nuclear modification effects, where $R_{\rm FB} = 1$, is 1.2%, corresponding to a deviation with a significance of 2.2σ. This measurement constitutes the first observation of Z boson production in proton-lead collisions.

6. Summary

Studies are performed of electroweak boson production at LHCb using data collected in 2011 at a centre-of-mass energy of 7 TeV. Measurements are presented of inclusive W boson production, as well as Z boson production in association with jets and D mesons. Additionally, the first measurement of Z boson production in proton-lead collisions is performed using a dataset collected in 2013 at $\sqrt{s_{NN}}$ = 5 TeV. Measurements are compared to theoretical calculations computed at up to NNLO in perturbative QCD and found to be in good agreement.

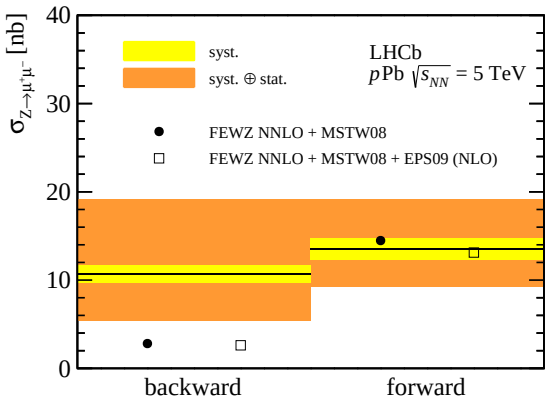

Figure 10: Experimental results compared to theoretical predictions for $Z \to \mu\mu$ production in proton-lead collisions for forward and backward events. The data is represented by the bands while the the theoretical predictions at NNLO with and without nuclear effects are indicated by the open and closed points respectively.

References

[1] J. Alves, A. Augusto, et al., The LHCb Detector at the LHC, JINST 3 (2008) S08005. doi:10.1088/1748-0221/3/08/S08005.

[2] LHCb collaboration, Measurement of the forward W boson cross-section in pp collisions at $\sqrt{s}$ = 7 TeV LHCb-CONF-2014-002.

[3] R. Aaij, et al., Inclusive W and Z production in the forward region at $\sqrt{s}$ = 7 TeV, JHEP 1206 (2012) 058. arXiv:1204.1620, doi:10.1007/JHEP06(2012)058.

[4] R. Aaij, et al., Measurement of the forward W boson cross-section in pp collisions at $\sqrt{s}$ = 7 TeVarXiv:1408.4354.

[5] R. Aaij, et al., Study of forward Z + jet production in pp collisions at $\sqrt{s}$ = 7 TeV, JHEP 1401 (2014) 033. arXiv:1310.8197, doi:10.1007/JHEP01(2014)033.

[6] M. Cacciari, G. P. Salam, G. Soyez, The Anti-k(t) jet clustering algorithm, JHEP 0804 (2008) 063. arXiv:0802.1189, doi:10.1088/1126-6708/2008/04/063.

[7] R. Aaij, et al., Observation of associated production of a Z boson with a D meson in the forward region, JHEP 1404 (2014) 091. arXiv:1401.3245, doi:10.1007/JHEP04(2014)091.

[8] R. Aaij, et al., Observation of Z production in proton-lead collisions at LHCb, JHEP 1409 (2014) 030. arXiv:1406.2885, doi:10.1007/JHEP09(2014)030.

[9] R. Gavin, Y. Li, F. Petriello, S. Quackenbush, FEWZ 2.0: A code for hadronic Z production at next-to-next-to-leading order, Comput.Phys.Commun. 182 (2011) 2388–2403. arXiv:1011.3540, doi:10.1016/j.cpc.2011.06.008.

[10] M. Hirai, S. Kumano, T.-H. Nagai, Determination of nuclear parton distribution functions and their uncertainties in next-to-leading order, Phys.Rev. C76 (2007) 065207. arXiv:0709.3038, doi:10.1103/PhysRevC.76.065207.